# Evaluation of fluorescent polysaccharide nanoparticles for pH-sensing†‡

**Anja Schulz,*[a] Stephanie Hornig,[b] Tim Liebert,[b] Eckhard Birckner,[a] Thomas Heinze[b] and Gerhard J. Mohr*[a]**

***Received 7th January 2009, Accepted 17th February 2009***
***First published as an Advance Article on the web 12th March 2009***
**DOI: 10.1039/b900260j**

The comprehensive characterization of novel dextran nanoparticles with regard to their suitability as pH-sensors for analytical applications (*e.g.* in physiology) is described. The nanoparticles are labeled with both a pH-indicator dye (fluorescein isothiocyanate, FITC) and a reference dye (sulforhodamine B acid chloride) as an internal standard. The fluorescence intensity of FITC increases with increasing pH, whereas the signal of the reference dye remains constant. Plotting the ratio of both signals against the pH gives a p$K_a$ of 6.45, which is appropriate for most of the measurement purposes. Furthermore, the influence of temperature, ionic strength and oxidizing substances on the performance of the fluorophores inside the dextran nanoparticles is examined. These results are compared to the dissolved dyes in order to evaluate if the dextran matrix affects the fluorescence properties of the sensor and the reference dye, and whether or not these nanosensors are suitable for pH-sensing in biological samples.

## Introduction

Monitoring pH in biological tissue or cells *via* fluorescence spectroscopy has become a widespread research area, including fluorescent nanoparticles with physically[1,2] or covalently entrapped dyes[3–6] and fiber-optics.[7,8] The nanosensors are based on materials such as polyacrylamide,[1,3,6,8] silica,[2] phospholipid-coated or amino-modified polystyrene[4,5] and methacrylate hydrogels.[7] Incorporation of the dyes in a polymer matrix avoids aggregation and compartmentalization, which may occur when using the plain fluorophores.[9] Furthermore, the biosamples are protected from mostly cytotoxic organic dyes.

Kopelman *et al.*[8] reported a fiber optic micro-sensor for physiological pH measurements, in which a fluorescein derivative is immobilized in a polyacrylamide matrix protecting the dye from undesired interactions with the biological sample. The micro-optode containing the dual-emission sensitive dye permits ratiometric measurements and shows fast response times as well as high sensitivity, operational lifetime and good reversibility. Although optodes are most suitable for physiological measurements, the applications are limited to tissue and sera because of the diameter of the fiber (2–250 μm). Measurements inside single cells are possible but the tip of the fiber can cause perturbation or damage to the cell. Embedding the sensing dyes in nanoparticles maintains the advantages of fiber-optics but profits from the small size of the beads. With particles in the nanometre range, high sensor loading rates and spatial distribution of the sensors inside the cell can be achieved. Furthermore, a high number of cells and various analytes can be examined simultaneously. Two approaches have been developed for the immobilization of dyes inside nanoparticles, *i.e.* physical entrapment of the fluorophores during the polymerization process and covalent attachment of dye derivatives to the particle matrix. The first method benefits from the easy nanosensor preparation where the particles can be loaded with commercially available indicator dyes. A drawback of physical dye immobilization is possible leaching of the fluorophores, which are toxic to the cell and can contaminate the biological sample. Additionally, leaching from the particles will cause changes in signal intensity leading to incorrect measurements. These problems can be overcome by embedding the dyes covalently. For that purpose a polymerizable derivative of the indicator dye has to be synthesized and furthermore co-polymerized during nanoparticle preparation. Although the synthesis of a polymerizable fluorophore is time-consuming and limits the number of suitable indicators, leaching of the dyes during measurement is minimized. This enhances the operational lifetime of nanosensors, their stability and provides stable measurement signals.

Almdal *et al.*[3] developed pH-sensitive ratiometric nanosensors in which both an indicator dye (fluorescein derivative) and a reference dye (rhodamine derivative) were covalently attached to a polyacrylamide matrix. The nanoparticles reversibly measured pH in the range from pH 5.8 to 7.2 and were therefore well suited for physiological applications. The polymer matrix composed of cross-linked polyacrylamide provided a hydrophilic environment which was beneficial for sensing in aqueous media (*e.g.* inside cells).

Another polymer highly appropriate for intracellular measurements is cellulose and its derivatives. The immobilization of indicator dyes to cellulose for sensing purposes[10,11] is well established. However, the use of dextran as the polymer matrix for optical sensors is less known. Although the polyglucan dextran is a widely used biopolymer in medical fields, the preparation of optical sensor layer or sensor nanoparticles is limited to a few examples.[12] The polysaccharide consists of α-1,6-glycosidically linked D-glucose units with varying branches depending on the dextran producing bacterial strain.[13] The esterification leads to

[a]*Institute of Physical Chemistry, Friedrich Schiller University of Jena, Germany. E-mail: Gerhard.Mohr@uni-jena.de; Fax: +49 3641 94 83 02; Tel: +49 3641 94 83 68*
[b]*Institute of Organic Chemistry and Macromolecular Chemistry, Friedrich Schiller University of Jena, Germany. E-mail: Thomas.Heinze@uni-jena.de; Fax: +49 3641 94 82 72; Tel: +49 3641 94 82 70*

† This paper is dedicated to Prof. Shinkai on the occasion of his 65th birthday.

‡ Electronic supplementary information (ESI) available: Spectra of the dyes, experimental details of time resolved fluorescence spectroscopy and calculations of FRET efficiency. See DOI: 10.1039/b900260j

 

hydrophobic dextran derivatives forming spherical nanoparticles with a narrow size distribution *via* dialysis of a *N*,*N*-dimethylacetamide (DMAc) solution against water.[14] The dextran matrix provides significant advantages over polystyrene, polyacrylamide or polymethacrylate such as high biocompatibility and non-toxicity. Functionalization of the dextran with dyes as well as adjustment of the hydrophilicity are easily achieved by substitution of the hydroxyl groups. Hence, a great variety of tailor-made polymers for specific applications becomes available. Special reagents or methods for particle delivery into the cytosol are unnecessary, because the particles are freely incorporated by the cells (*e.g.* fibroblasts[12]) probably *via* endocytosis. Due to their biocompatibility, the intracellular analysis is truly non-invasive.

In the present paper, we describe the characterization of dextran nanoparticles that have been covalently labeled with an indicator and a reference dye to enable stable measurements of pH, in particular in biological media. The sensor particles are tested towards interferences with substances that can occur in buffer media used for physiological examinations. Thus, cross-reactivity of the free and incorporated dyes to ionic strength is investigated and compared. The characteristics of the dyes towards fluorescence resonance energy transfer (FRET), autoclaving, oxidation, changes in light source intensity and photostability were investigated as well. In this manner it can be verified whether or not the dextran matrix has an influence on the optical and physico-chemical properties of the dyes incorporated inside the particles.

## Results and discussion

The esterification of dextran leads to hydrophobic polymers, *e.g.* propionylated dextrans, which are capable of forming well defined nanospheres with a narrow size distribution. The covalent attachment of fluorescent dyes can be carried out either before or after propionylation to prevent undesired acid catalyzed hydrolysis of the dyes. Because fluorescence spectroscopy is a highly sensitive measuring method, only low degrees of substitution with dyes ($DS_{FITC}$: 0.0265; $DS_{SRB}$: 0.00145) are necessary minimizing intra- and intermolecular interactions. The functionalization of dextran with SRB acid chloride and subsequent perpropionylation leads to a completely substituted SRB labeled dextran propionate (SRB-dextran propionate), which is used as a reference system. The pH indicator dye fluorescein isothiocyanate was allowed to react with a dextran propionate possessing a degree of substitution of 1.81 (FITC-dextran propionate).

The dialysis of a DMAc solution containing both SRB-dextran propionate and FITC-dextran propionate against water led to dextran nanoparticles. The spheres are 680 nm in size and exhibit a polydispersity index (PDI) of 0.256 as examined by dynamic light scattering (DLS).

The excitation and emission spectra of FITC and SRB in solution as well as incorporated inside the sensor particles are depicted in Fig. 1.

It can be seen that incorporation of the dyes inside the dextran matrix has no major effect on the fluorescence spectra of the fluorophores. Excitation and emission maxima for free FITC and incorporated FITC are at 490 nm and 516 nm, respectively. The excitation maximum of the reference dye SRB is at 561 nm

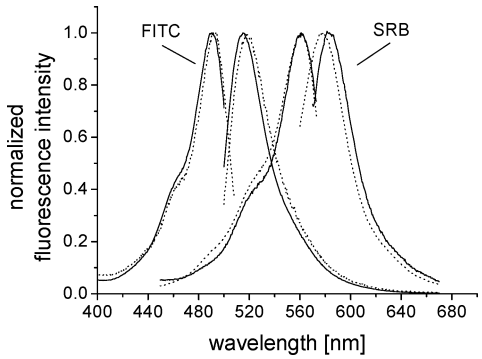


**Fig. 1** Normalized fluorescence excitation and emission spectra of FITC and SRB in buffered solution of pH 7.2 (dotted line) and incorporated inside nanosensors (solid line) suspended into buffer pH 7.2.

for the dye in solution as well as for the labeled dextran. The maximum of fluorescence emission is slightly shifted from 578 nm to 584 nm upon incorporation of the fluorophore inside the nanoparticles.

A major part of the ratiometric fluorescent sensors that can be found in the literature uses a combination of fluorescein dyes and rhodamines to monitor changes in pH. Although it is also known that fluoresceins and rhodamines are suitable donor–acceptor pairs for fluorescence resonance energy transfer (FRET), this fluorophore combination is still very popular. This may be due to the commercial availability of many fluorescein and rhodamine derivatives and the compatibility of the excitation wavelengths with laser excitation sources. Furthermore, fluorescein has a relevant $pK_a$ and shows strong signal changes. Despite the popularity of this fluorophore system, to date an evaluation of the FRET characteristics between fluorescein and rhodamine inside polymer nanoparticles is still missing. There are a few articles describing *e.g.* FRET between fluorophores like perylene, coumarin 6 and nile red in polyfluorene nanoparticles[15] or the influence of fluorescein adsorption on rhodamine doped microparticles.[16] In the following, two methods are employed to assess the FRET efficiency of FITC and SRB inside dextran nanoparticles.

To evaluate if there is any FRET between FITC (donor) and SRB (acceptor) inside the particles, both the Förster radius ($R_0$) between the dyes and the distance of the dyes inside the nanoparticle had to be calculated. Due to the strong scattering in the nanoparticle suspension, it was not possible to obtain an absorbance spectrum of SRB immobilized in the particles. Consequently, the Förster radius was calculated from the spectra obtained in solution, because the absorbance spectrum of the acceptor dye was needed. For the FITC–SRB donor–acceptor pair, a Förster radius of $R_0 = 46$ Å (in 0.1 N NaOH) was determined (see ESI‡). Comparable radii can be found in the literature[17] for similar donor–acceptor pairs (*e.g.* for FITC–tetramethylrhodamine, $R_0 = 49$–$54$ Å).

The theoretical fluorophore loading was calculated using the degree of substitution of the dextran derivatives. Therefore, the average distance between the fluorophores inside the nanosensor was estimated according to Almdal *et al.*[3] (see ESI). Thus, the mean distance ($R$) between the dye molecules inside the particles was assessed to be around 56 Å. The ratio of the distance between the dye molecules and the Förster radius was used to calculate

the efficiency ($E$) of the energy transfer (eqn (1)), which here was about 23%.

$$E = \frac{1}{\left(R/R_0\right)^6 + 1} \quad (1)$$

Due to the sixth power in the term ($R/R_0$) the transfer efficiency strongly depends on the distance between donor and acceptor. Hence, the accuracy of this theoretical FRET efficiency is limited by the rough estimation of this distance $R$ between both dyes in the particles. Therefore, an experimental method for determination of energy transfer efficiency was applied to verify the calculations. The fluorescence lifetime of FITC inside nanoparticles containing only FITC ($\tau_D$) was measured as well as FITC lifetime in particles containing additionally the acceptor fluorophore SRB ($\tau_{DA}$). For that purpose, FITC/SRB-labeled particles with three different donor–acceptor compositions were prepared.

The FITC-labeled nanoparticles show a bi-exponential fluorescence decay with a major component ($\Phi_1 = 84\%$) of $\tau_1 = 4.0$ ns and a minor contribution ($\Phi_2 = 16\%$) of $\tau_2 = 1.5$ ns. Inside the FITC/SRB-labeled beads, the fluorescence lifetime of FITC follows a bi-exponential decay as well. The lifetime of the donor is reduced to $\tau_1 \approx 3.6$ ns and $\tau_2 \approx 1.2$ ns for all three donor–acceptor compositions. The lifetime of FITC inside the labeled particles is the same for all different compositions due to nearly equal concentrations of acceptor fluorophore (Table 1). The bi-exponential fluorescence decay and the appearance of a slow $\tau_1$ and a fast $\tau_2$ for incorporated FITC is in good agreement with data obtained from labeled silica nanoparticles.[18]

The FRET efficiency $E$ is calculated (eqn (2)) using the ratio of fluorescence lifetimes between the donor alone ($\tau_D$) and the donor in presence of acceptor ($\tau_{DA}$).[19]

$$E = 1 - \frac{<\tau_{DA}>}{<\tau_D>} \quad (2)$$

With E ≈ 30%, the experimentally determined transfer efficiency is in the same range as the calculated one (E = 23%) and thus verifies the results obtained from calculation. Although the accuracy of these methods is limited, it shows that both ways are suitable for estimation of the FRET efficiency inside the particles. The efficiency of around 30% for the energy transfer between donor and acceptor dye is considerable, but as seen from the following examinations, it seems to have no significant negative influence on the performance of pH measurements.

### pH-Sensitivity of the dyes in solution and immobilized inside the particles

The ratio between the pH-dependent fluorescence of FITC and the fluorescence of the reference dye (SRB acid chloride, pH insensitive fluorophore) was plotted against pH. The acidity constant was determined by fitting a calibration curve to the experimental data according to the function:

$$S = \frac{\left(A + B \cdot K_a \cdot 10^{pH}\right)}{\left(1 + K_a \cdot 10^{pH}\right)},$$

where $S$ is the fluorescence signal ratio, $A$ the estimated lower limit of the calibration graph and $B$ the upper limit, respectively. The absorbance and emission spectra of both FITC and SRB in phosphate buffer solution (PBS) with varying pH are shown in Fig. 2.

In solution, the intensity of the emission maximum (516 nm) increased about 18-fold when increasing the pH of the buffer from 5.0 to 8.0 resulting in a p$K_a$ of 6.38 ± 0.02. The incorporation of fluorescein isothiocyanate into the dextran matrix did not significantly affect the fluorescence excitation and emission maxima. After FITC was covalently linked to the dextran nanoparticles, the increase in intensity within the pH-range 5 to 8 was lowered to 11-fold. The p$K_a$ of FITC slightly changed to higher values (p$K_a$ 6.45 ± 0.03) due to immobilization inside the polymer (Fig. 3).

The sensitivity of the sensor particles was determined to be in the range between pH 5.7 and 7.1 and thus matches the relevant biological measuring conditions. The intensity of the excitation and emission maximum of SRB was neither affected in solution nor inside the particles as pH was increased from 5 to 8.

As illustrated in Fig. 4, the dextran nanoparticles as well as the immobilized dyes were stable during standard sterilizing procedures for 2 h at 120 °C and 2 bar in an autoclave.

### Cross-reactivity to ionic strength

The influence of ionic strength (IS) on fluorescence of the dissolved dyes and the nanosensors was investigated using sodium chloride as the background electrolyte.

Fig. 5a shows the calibration graphs of the dyes in PBS containing 0, 100 and 200 mM sodium chloride. The p$K_a$ of FITC in buffer with the highest IS was shifted by about 0.18 units to give 6.2.

The sensor nanoparticles exhibited nearly the same decreases in p$K_a$ by about 0.19 units, if calibrated in phosphate buffer with

**Table 1** Fluorescence lifetimes ($\tau_1$, $\tau_2$) with relative contribution ($\Phi_1$, $\Phi_2$) to the quantum yield ($\Phi_f$) of FITC in solution (0.1 N NaOH), FITC-labelled nanoparticles (NP) and FITC/SRB-labelled nanoparticles in suspension adjusted to pH 11 with 0.1 N NaOH. E is the experimental energy transfer efficiency calculated from the lifetimes according to eqn (2) and $R_{exp}$ is the experimentally determined distance between the fluorophores

| | $\tau_1$ [ns] | $\Phi_1$ | $\tau_2$ [ns] | $\Phi_2$ | $<\tau>$ [ns][d] | $\Phi_f$ | E | $R_{exp}$ [Å][e] |
|---|---|---|---|---|---|---|---|---|
| FITC (solution) | 2.7 | 15 | 0.55 | 85 | 0.62 | 0.07 | — | — |
| FITC (NP) | 4.0 | 84 | 1.5 | 16 | 3.2 | 0.17 | — | — |
| FITC/SRB (NP)[a] | 3.8 | 65 | 1.4 | 35 | 2.4 | — | 0.25 | 55 |
| FITC/SRB (NP)[b] | 3.6 | 70 | 1.1 | 30 | 2.1 | — | 0.34 | 51 |
| FITC/SRB (NP)[c] | 3.6 | 72 | 1.2 | 28 | 2.3 | — | 0.28 | 54 |

[a] Ratio of FITC/SRB = 0.49. [b] Ratio of FITC/SRB = 0.94. [c] Ratio of FITC/SRB = 1.64. [d] $<\tau> = 100\%/(\Phi_1/\tau_1 + \Phi_2/\tau_2)$. [e] $R_{exp} = R_0\ ((1\text{-}E)/E)^{1/6}$ with $R_0 = 46$ Å.

 

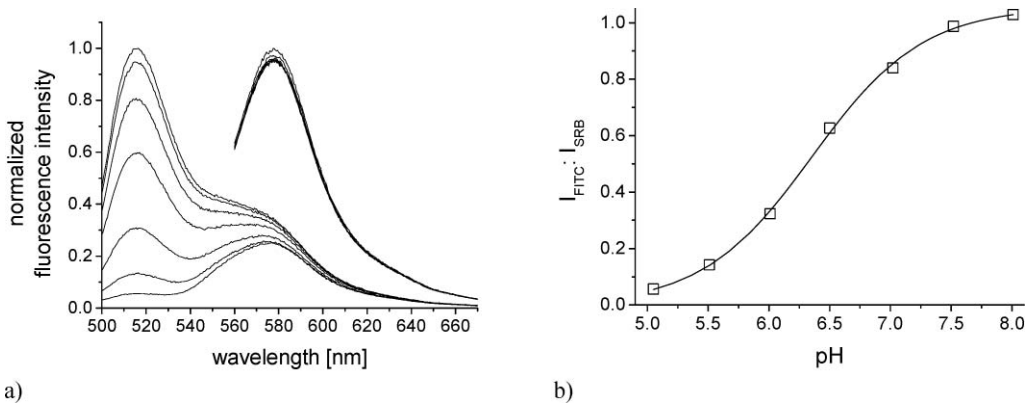


**Fig. 2** (a) Normalized fluorescence emission spectra of FITC and SRB (mSRB : mFITC = 8) dissolved in PBS with pH rising from 5.0 to 8.0. (b) Ratio of fluorescence intensities of the dyes in solution and fitted calibration graph.

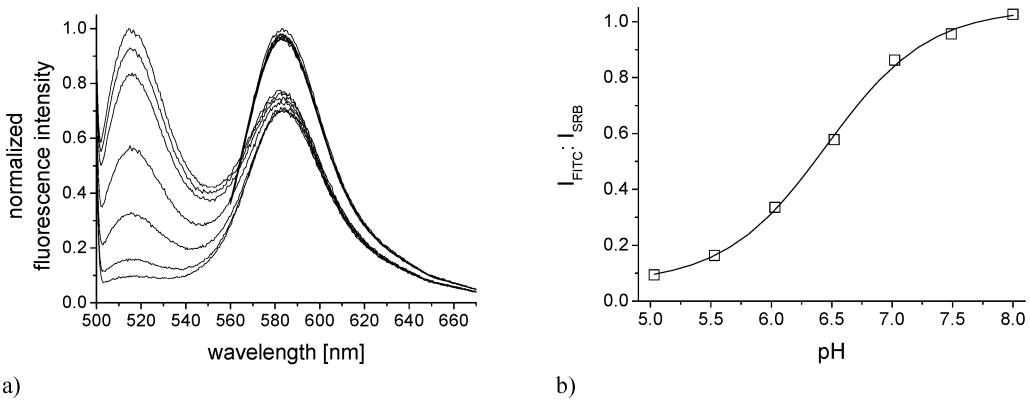


**Fig. 3** (a) Normalized fluorescence emission spectra of FITC and SRB (mSRB : mFITC = 7) immobilized inside dextran nanoparticles suspended in buffer solution with pH rising from 5.0 to 8.0. (b) Ratio of fluorescence intensities of the incorporated dyes and fitted calibration graph.

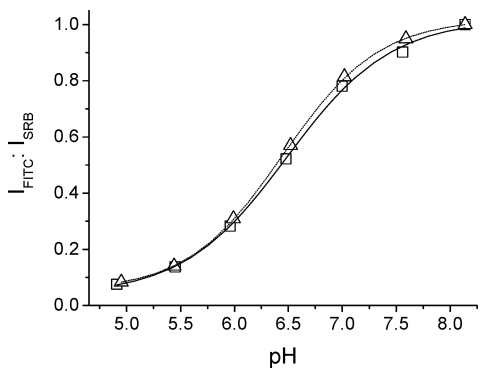


**Fig. 4** Calibration plots of the dextran nanoparticles before (□) and after (△) sterilization at 2 bar and 120 °C.

200 mM of sodium chloride added (Fig. 5b). The ionic strength affected the p$K_a$ of both FITC in solution as well as inside the particles due to the negative charge of the dye, which is present as the mono- and dianion form.[20] Immobilization of the indicator dye in the dextran particles did not alter this response to ionic strength and thus an effect of the matrix can be precluded. For application of the nanosensors, the ionic strength of the buffer media has to be considered during calibration.

### Oxidation of the dyes

For application of the nanosensors in biological samples, the effect of intracellular substances like enzymes has to be taken into consideration. Enzymes are known to be capable of catalyzing oxidation processes (*e.g.* monooxygenases). For that purpose, the plain dyes and the dextran nanoparticles in PBS were investigated towards oxidation by hydrogen peroxide.

We found that FITC dissolved in PBS of pH 8.0 was oxidized by hydrogen peroxide. When exposed to concentrations up to 145 mM $H_2O_2$, the fluorescence intensity immediately decreased by about 11%. In contrast, FITC embedded in dextran showed a negligible increase in fluorescence intensity by about 3% upon exposure to 145 mM $H_2O_2$. The emission of SRB remained constant in the presence of hydrogen peroxide. Thus, in the case of oxidation processes, the dextran matrix exhibited a protective effect on the incorporated dyes compared to the dyes in solution.

### Influence of light source intensity

For practical application of the nanosensors, it is necessary to show that the ratio of fluorescence intensities of both dyes is independent from the intensity of the light source and the sensitivity of the detector. Such fluctuations were simulated by changing the width of the excitation and emission bandpasses of the fluorescence spectrometer.

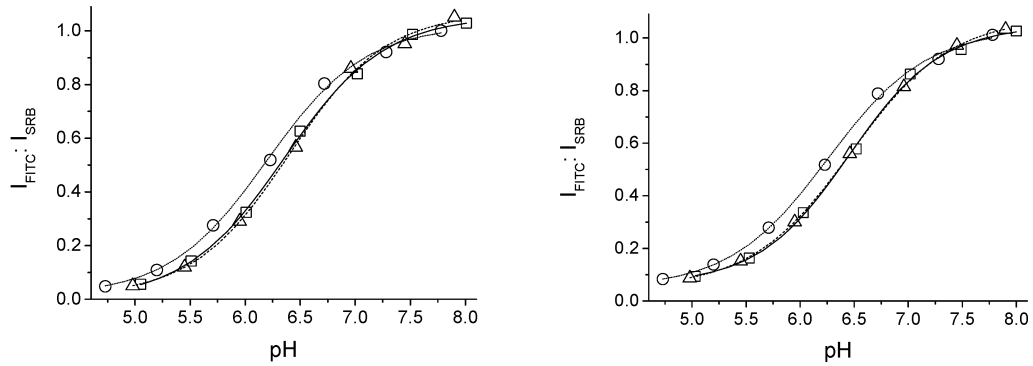


**Fig. 5** Ratio of fluorescence intensities and fitted calibration graph of (a) the dyes dissolved in phosphate buffer solution, and (b) the dyes immobilized in nanoparticles and suspended in phosphate buffer of rising ionic strength: 0 mM NaCl (□), 100 mM NaCl (△) and 200 mM NaCl (○).

If only the emission of FITC was detected, a change in width of the excitation slit dramatically changed the intensity of the emitted fluorescence (about 10-fold) as depicted in Fig. 6. If the emission intensity of FITC was divided by the intensity of SRB, then the obtained ratio of the fluorescence was nearly the same. The determined p$K_a$ values for different excitation and emission bandpasses varied only by 0.02 (6.45 at slit 4/4, 6.44 at slit 6/2 and 6.43 at slit 6/6). The combination of both fluorescent indicator and reference dyes, allowing the ratiometric detection of analytes, is an important contribution to stable and reliable measurements. Changes in fluorescence intensity of the indicator dye are only caused by the analyte and effects caused by spatial motion of the sensor nanoparticles or fluctuations in the light source intensity can be precluded.

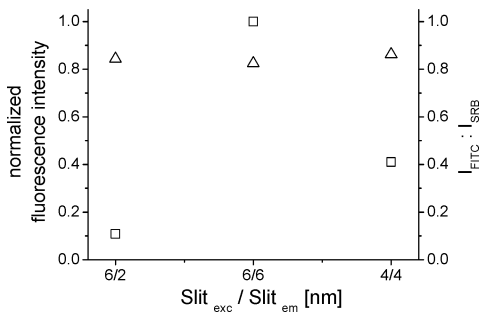


**Fig. 6** Changes of FITC fluorescence intensity due to changes in light source intensity (□) and stable fluorescence signals obtained by calculation of the signal ratio using a reference dye (△).

### Photobleaching of the dyes

For physiological measurements, dyes are required that are stable against irradiation by light of high intensity, *e.g.* lasers, which are common excitation light sources. To examine how fluorophores are affected by light of high intensity, a cuvette with both dyes was exposed to the excitation light source (450 W xenon lamp) in the fluorescence spectrometer.

After 10, 60 and 140 min respectively, fluorescence spectra were recorded. It can be seen that FITC in solution as well as inside the dextran nanoparticles showed a significant decrease in fluorescence intensity after 10 min of irradiation (Fig. 7). After

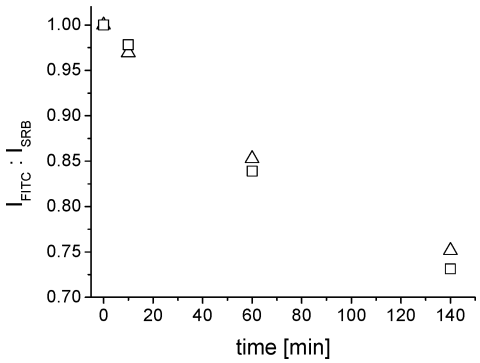


**Fig. 7** Photobleaching of FITC embedded inside dextran nanosensors (□) compared to FITC in solution (△) after 10, 60 and 140 min of irradiation.

140 min, the intensity of the plain FITC decreased by about 21% and that of the entrapped one by about 28%. The enhanced decomposition of the particle-incorporated FITC is related to the lower mobility of the dye inside the polymer matrix and of the particles in the aqueous suspension. As expected, SRB fluorescence showed no photobleaching even after a period of 140 min irradiation. Experiments can take longer than 140 minutes and bleaching of FITC may result in a strong impact on the measurements. As a consequence, we are currently developing pH indicator dyes with similar pH-sensitivity but significantly enhanced photostability.

## Conclusion

In summary, novel pH-nanosensors are characterized in terms of fluorescence lifetime, autoclaving stability, response to ionic strength, oxidation and photobleaching. The shortened fluorescence lifetime of incorporated FITC in presence of SRB indicates that energy transfer takes places. However, while the type and extent of energy transfer is difficult to determine, no negative influence on the performance of pH measurements is observed. The dextran nanoparticles exhibit a p$K_a$ of 6.45, which corresponds very well with that of the unbound FITC (6.38). Despite the low cross-sensitivity to ionic strength, the calibration of the particles has to be performed with respect to IS of the

 

buffer media. The oxidation of the dyes due to hydrogen peroxide is prevented *via* immobilization inside the polymer particles. It is shown that signal changes, which are not caused by the analyte such as fluctuations in light source intensity, can be precluded. For application of the nanosensor in real samples, the photostability of the FITC limits the lifetime of the nanosensors and new fluorescent indicator dyes have to be developed.

## Experimental section

### Apparatus

The fluorescence spectra were recorded in a 10 mm cuvette on a Fluorolog 3 from Jobin Yvon-Spex at a temperature of (25 ± 1) °C. The fluorescence kinetics were measured with the time-correlating single photon counting spectrometer CD900 (Edinburgh Instruments), see ESI.‡ The wavelength for excitation of the dyes in solution as well as for the nanosensors was 489 nm for fluorescein isothiocyanate and 543 nm for the reference dye, respectively. For characterization of the particles with fluorescence spectrometry, 0.1 mL of a dialyzed particle suspension (1 mg nanoparticles per mL) was added to 2 mL of phosphate buffer solution in a cuvette.

The particle size and the zeta potential of the nanospheres were determined by dynamic light scattering (DLS) studies using a laser beam at 633 nm and a scattering angle of 173° (Zetasizer Nano ZS, Malvern Instruments).

### Materials

Sodium chloride, sodium hydroxide, hydrogen peroxide (30%), disodium hydrogen phosphate monohydrate, dextran, fluorescein 5(6)-isothiocyanate (FITC), sulforhodamine B acid chloride (SRB) and sodium dihydrogen phosphate dihydrate were obtained from Fluka.

Dextran with the weight-average molecular weight of 54 800 g $mol^{-1}$ and a polydispersity index (PDI) of 1.56 produced by *Leuconostoc mesenteroides* strain no. NRRL B-512(F) was purchased from Fluka.

For the preparation of buffer solutions, double-deionized water (conductivity $\leq$0.055 μS $cm^{-1}$) was used. Phosphate buffers were prepared by mixing 67 mM aqueous solutions of sodium dihydrogen phosphate hydrate and disodium hydrogen phosphate dihydrate until the desired pH was achieved. The pH was controlled with a digital pH meter from Hanna Instruments and calibrated at 25 ± 1 °C with standard buffers of pH 4.0 and pH 7.0 (Merck).

### Synthesis of dextran nanoparticles

The preparation of the labeled dextran nanoparticles is described in a previous publication.[12] In brief, dextran was propionylated using propionic acid anhydride and labeled with FITC and SRB acid chloride. The degree of substitution of the dextran with these dyes was determined using UV/Vis-spectroscopy in the case of SRB-dextran and *via* fluorescence spectroscopy for the FITC-derivative. The preparation of the nanoparticles was carried out by a dialysis process. A total quantity of 20 mg of dextran ester (a mixture of FITC-dextran propionate and SRB-dextran propionate at a weight ratio of 1 : 7) was dissolved in 5 mL purified *N*,*N*-dimethylacetamide (DMAc) and dialyzed against distilled water (Spectra/Por® membrane, molecular weight cut-off 3500 g $mol^{-1}$) for 4 d. The deionized water was exchanged 5 times in intervals of at least 3 hours.


## Acknowledgements

This work was supported by research grants MO 1062/5-1 and MO 1062/6-1 of Deutsche Forschungsgemeinschaft and by the European Union project "Sensor Nanoparticles for Ions and Biomolecules" (MTKD-CT-2005-029554). This support is most gratefully acknowledged.


## Notes and references


1 H. A. Clark, R. Kopelman, R. Tjalkens and M. A. Philbert, *Anal. Chem.*, 1999, **71**, 4837.
2 J. Peng, X. He, K. Wang, W. Tan, Y. Wang and Y. Liu, *Anal. Bioanal. Chem.*, 2007, **388**, 645.
3 H. Sun, A. M. Scharff-Poulsen, H. Gu and K. Almdal, *Chem. Materials*, 2006, **18**, 3381.
4 K. P. McNamara, T. Nguyen, G. Dumitrascu, J. Ji, N. Rosenzweig and Z. Rosenzweig, *Anal. Chem.*, 2001, **73**, 3240.
5 J. Ji, N. Rosenzweig, C. Griffin and Z. Rosenzweig, *Anal. Chem.*, 2000, **72**, 3497.
6 K. Almdal, H. Sun, A. K. Poulsen, L. Arleth, I. Jakobsen, H. Gu and A. M. Scharff-Poulsen, *Polym. Adv. Technol.*, 2006, **17**, 790.
7 P. A. Wallace, N. Elliott, M. Uttamlal, A. S. Holmes-Smith and M. Campbell, *Meas. Sci. Technol.*, 2001, **12**, 882.
8 A. Song, S. Parus and R. Kopelman, *Anal. Chem.*, 1997, **69**, 863.
9 O. Seksek, N. Henry-Toulmé, F. Sureau and J. Bolard, *Anal. Biochem.*, 1991, **193**, 49.
10 G. J. Mohr and O. S. Wolfbeis, *Anal. Chim. Acta*, 1994, **292**, 41.
11 T. Carofiglio, C. Fregonese, G. J. Mohr, F. Rastrelli and U. Tonellato, *Tetrahedron*, 2006, **62**, 1502.
12 S. Hornig, C. Biskup, A. Graefe, J. Wotschadlo, T. Liebert, G. J. Mohr and T. Heinze, *Soft Matter*, 2008, **4**, 1169.
13 T. Heinze, T. Liebert, B. Heublein and S. Hornig, *Adv. Polym. Sci.*, 2006, **205**, 199.
14 T. Liebert, S. Hornig, S. Hesse and T. Heinze, *J. Am. Chem. Soc.*, 2005, **127**, 10484.
15 C. Wu, Y. Zheng, C. Szymanski and J. McNeill, *J. Phys. Chem. C*, 2008, **112**, 1772.
16 F. Caruso, E. Donath and H. Möhwald, *J. Phys. Chem. B*, 1998, **102**, 2011.
17 P. Wu and L. Brand, *Anal. Biochem.*, 1994, **218**, 1; D. A. Johnson, J. G. Voet and P. Taylor, *J. Biol. Chem.*, 1984, **259**, 5717; D. Kosk-Kosicka, T. Bzdega and A. Wawrzynow, *J. Biol. Chem.*, 1989, **264**, 19495.
18 S. Santra, B. Liesenfeld, C. Bertolino, D. Dutta, Z. Cao, W. Tan, B. M. Moudgil and R. A. Mericle, *J. Luminescence*, 2006, **117**, 75.
19 J. R. Lakowicz, in *Principles of Fluorescence Spectroscopy 2nd edition*, Kluwer Academic/Plenum Publishers, New York, 1999.
20 B. M. Weidgans, C. Krause, I. Klimant and O. S. Wolfbeis, *Analyst*, 2004, **129**, 645.